Diterpenoid and Flavonol Glycosides from Sumatran Fern *Selliguea feei* Bory

Arif Ferdian[1],[2], Nova Syafni[1], Deddi Prima Putra[1], and Dayar Arbain[1*]
[1]Department of Pharmacy
Universitas Andalas
Padang, 25163, Indonesia

[2]Department of Clinical Pharmacy
Universitas Baiturrahmah
Padang, 25176, Indonesia
**dayararbain@gmail.com*

Date received: September 12, 2025
Revision accepted: October 26, 2026

Abstract

Selliguea feei Bory (Polypodiaceae) is a Sumatran fern whose rhizomes are traditionally used to treat rheumatism and hypertension. However, its fronds have not previously been chemically investigated, and none of its constituents have been evaluated against multidrug-resistant bacteria. This study aimed to isolate and characterize secondary metabolites from the fronds of S. feei and to evaluate their antibacterial activity against clinical isolates of methicillin-resistant Staphylococcus aureus (MRSA) and multidrug-resistant Pseudomonas aeruginosa (MDRPA). Fresh fronds were macerated with methanol and successively partitioned with n-hexane, ethyl acetate, and n-butanol. The ethyl acetate and n-butanol fractions were separated using silica gel column chromatography and crystallization. Structures were elucidated using 1D and 2D NMR, UV–Vis, IR, and LC–MS analyses. Antibacterial activity was determined using the agar diffusion method at 60 µg/disc, with chloramphenicol (3 µg/disc) as the positive control. Four known compounds were isolated: the diterpenoid onychiol B (1) and three flavonol glycosides, kaempferol-7-O-α-L-rhamnoside (2), kaempferol-3,7-O-α-L-dirhamnoside (3), and kaempferol-3-O-β-D-glucoside-7-O-α-L-rhamnoside (4). Compounds 1–3 are reported for the first time from the genus Selliguea. Compound 2 showed moderate inhibition of MRSA (12.17 ± 0.88 mm) and limited inhibition of MDRPA (6.92 ± 0.14 mm).

***Keywords**:* diterpenoid, flavonol glycoside, methicillin-resistant *Staphylococcus aureus*, multidrug-resistant *Pseudomonas aeruginosa*, *Selliguea feei*

1. Introduction

Selliguea feei Bory (*Polypodiaceae*) is a fern species distributed in volcanic montane forests of Indonesia and the Philippines. In Indonesia, particularly in West Java, the rhizomes of this plant have been used in traditional medicine to treat rheumatism and hypertension, indicating its potential pharmacological relevance. These ethnopharmacological applications have prompted phytochemical investigations aimed at identifying bioactive constituents that may serve as leads for drug development (Subarnas & Wagner, 2000).

Previous studies on *S. feei* have focused predominantly on its rhizome and have reported several secondary metabolites, including the proanthocyanidins selligueain A and selligueain B; the flavonoid glycosides (+)-afzelechin-)-*O*-β-4′-D-glucopyranoside and kaempferol-3-*O*-β-D-glucopyranoside-7-*O*-α-L-rhamnopyranoside; and (−)-4-β-carboxymethyl epiafzelechin-(3′-deoxydryopteric acid) (Baek *et al*., 1993; Baek *et al*., 1994). However, no comprehensive phytochemical investigation has been conducted on the fronds of this species. Because distinct plant organs often exhibit unique metabolic profiles, the lack of chemical data on the fronds represents an important knowledge gap. Furthermore, most studies to date have evaluated antibacterial activity against standard reference strains rather than clinically relevant multidrug-resistant bacteria, thereby limiting the translational relevance of existing findings.

Despite previous phytochemical studies of the rhizomes of *S. feei*, the chemical constituents of its fronds remain largely unexplored, and no study has evaluated the bioactivity of isolated compounds from the fronds against clinically relevant multidrug-resistant pathogens. In continuation of our ongoing investigation of Sumatran ferns (Syafni *et al*., 2012; Anggia *et al*., 2015; Nofrizal *et al*., 2017), the present study was undertaken to address this gap. The objective was to isolate and characterize secondary metabolites from the fronds of *S. feei* and evaluate the antibacterial activities of the isolated compounds against two clinically important multidrug-resistant pathogens: methicillin-resistant *Staphylococcus aureus* (MRSA) and multidrug-resistant *Pseudomonas aeruginosa* (MDRPA).

2. Methodology

2.1 Plant Material

The fronds of *S. feei* were collected from the crater of Mount Tandikek at an elevation of 2,400 m above sea level in West Sumatra. Samples were collected on December 26, 2016. A voucher specimen (AF0001) was identified and deposited at Herbarium ANDA, Department of Biology, Faculty of Mathematics and Natural Sciences, Universitas Andalas. The collection site lies outside conservation areas and protected forest areas, and *S. feei* is not listed as a protected species under Indonesian regulations; no collection permit was therefore required. The plant material was collected in accordance with the applicable national regulations on the utilization of plant genetic resources. The study did not involve human subjects or animals, and no ethical approval was required.

2.2 General Procedure

Deuterated solvents (CD_3OD and DMSO-d_6) for NMR (ARMAR Chemicals, Switzerland). Solvents used for extraction, column chromatography, and crystallization were technical grade (Merck, Germany) and were distilled before use. Column chromatography was performed using silica gel 60 (0.040–0.063 mm; Merck, Germany). TLC analyses were performed using silica gel 60 F_{254} plates (Merck, Germany).

Antibacterial assays were performed using a local isolate of methicillin-resistant *S. aureus* (MRSA; Cipto Mangunkusumo Hospital, Jakarta, Indonesia) (Handayani *et al*., 2023) and multidrug-resistant *P. aeruginosa* (MDRPA; M. Djamil Hospital, Padang, Indonesia). Each bacterial strain was grown separately on nutrient agar (NA; Merck, Germany). A single clinical isolate of each organism was used. Both isolates were obtained as characterized multidrug-resistant strains from the clinical microbiology laboratories of the hospitals named above and were not isolated by the authors. Primary identification and antimicrobial susceptibility testing, including confirmation of methicillin resistance in *S. aureus* and of the multidrug-resistant phenotype in *P. aeruginosa*, were performed by those laboratories as part of their routine diagnostic work following CLSI criteria. Isolate identification codes and the corresponding resistance profiles were not released to the authors, which is acknowledged as a limitation of the present study.

UV spectra were measured using a spectrophotometer UV–Vis (Genesys 10S, Thermo Scientific, USA). IR spectra were recorded using a Shimadzu IR spectrophotometer (IRPrestige-21, Shimadzu, Japan) with KBr. NMR spectra were recorded at 500 MHz for ^{1}H NMR and 125 MHz for ^{13}C NMR using an Avance III instrument (Bruker, Germany). MS analyses were performed using LC–PDA–MS/MS (ESI LCMS-8030; Shimadzu, Japan).

2.3 Extraction and Isolation

Fresh fronds of *S. feei* (1.3 kg) were chopped into small pieces and macerated with methanol three times for 3 days per extraction at room temperature. The combined solvents were evaporated *in vacuo* to yield the methanolic extract (160 g). Distilled water was added to a final volume of 1 L, and the aqueous mixture was then successively partitioned with *n*-hexane, ethyl acetate (EtOAc), and *n*-butanol (BuOH). The solvents were evaporated *in vacuo* to yield the *n*-hexane (17.50 g, 10.9% of the crude extract), EtOAc (45.95 g, 28.7%), and BuOH (52.00 g, 32.5%) fractions. The aqueous phase remaining after partitioning was not concentrated or weighed, and its mass is therefore not reported; the three organic fractions together account for 72.2% of the 160 g methanolic extract, the balance corresponding to this aqueous fraction together with losses during transfer and solvent removal. The EtOAc fraction was subjected to silica gel column chromatography and eluted using a stepwise polarity gradient with increasing amounts of EtOAc in *n*-hexane, followed by increasing amounts of MeOH in EtOAc, to obtain seven major subfractions, A–G. Subfraction E was evaporated and crystallized from EtOAc–*n*-hexane to yield colorless needles of compound 1 (onychiol B; 700 mg; m.p. 198.5 °C). Subfraction F (500 mg) was further purified by column chromatography using a stepwise polarity gradient with increasing amounts of MeOH in EtOAc to yield four subfractions, F1–F4. Subfraction F1 was evaporated and crystallized from EtOAc–*n*-hexane to yield yellow needles of compound 2 (kaempferol-7-*O*-α-L-rhamnoside; 60 mg; m.p. 180–185 °C). Subfraction G was evaporated and crystallized from MeOH–$CHCl_3$ to yield yellow needles of compound 3 (kaempferol-3,7-*O*-α-L-dirhamnoside; 180 mg; m.p. 202–203 °C).

The BuOH fraction was subjected to silica gel column chromatography using silica gel as the stationary phase and a stepwise polarity gradient with increasing amounts of MeOH in EtOAc to yield seven major subfractions, 1–7; subfraction 4 was evaporated and crystallized from MeOH to yield a yellow amorphous solid identified as compound 4

(kaempferol-3-*O*-β-D-glucoside-7-*O*-α-L-rhamnoside; 77 mg; m.p. 238–240 °C).

2.4 Antibacterial Assays

Antibacterial activity was evaluated using a modified Kirby–Bauer agar disc diffusion method (Valgas *et al*., 2007). Before testing, each bacterial strain was grown separately on nutrient agar (NA; Merck, Germany) and incubated at 37 °C for 24 h. Culture suspensions were prepared in sterile 0.9% NaCl, adjusted to 25% transmittance, and swabbed onto the surfaces of NA plates. The isolated compounds were dissolved in DMSO at a concentration of 6 mg/mL. An aliquot of 10 µL of each solution was applied to a paper disc (6 mm diameter; Advantec, Japan), corresponding to a final load of 60 µg/disc, and the discs were carefully placed onto the inoculated agar surfaces. Positive-control discs were prepared in the same manner using chloramphenicol solution (300 µg/mL in DMSO; 3 µg/disc), whereas discs loaded with 10 µL of DMSO alone served as negative controls. The plates were incubated at 37 °C for 24 h, after which the inhibition zones, including the 6 mm disc diameter, were measured using a caliper. All assays were performed in triplicate using three separate Petri dishes, and the results are expressed as the mean ± standard deviation (SD) of three replicates.

3. Results and Discussion

The present investigation characterized the chemical constituents of the fronds of *S. feei* and yielded one diterpenoid [onychiol B (700 mg; m.p. 198.5 °C), compound 1] and three flavonol glycosides [compound 2 (60 mg; m.p. 180–185 °C), compound 3 (180 mg; m.p. 202–203 °C), and compound 4 (77 mg; m.p. 238–240 °C)]. Structural confirmation using comprehensive spectroscopic approaches, including 1D and 2D NMR, LC–MS, UV, and IR analyses, demonstrated strong agreement with previously published data. Importantly, compounds 1–3 are reported here for the first time from the genus *Selliguea*, thereby expanding knowledge of the chemotaxonomy of Polypodiaceae ferns.

Compound 1 was obtained as colorless needles. Its positive-ion LC–MS spectrum did not show the protonated molecule at *m/z* 321; instead, the base peak appeared at *m/z* 303.25, corresponding to $[M + H - H_2O]^+$, whereas the

dimeric ion at *m/z* 641.35 was consistent with [2M + H]+, confirming a molecular weight of 320 and the molecular formula $C_{20}H_{32}O_3$, corresponding to five degrees of unsaturation (Liao *et al.*, 2023). The absence of $[M + H]^+$ is consistent with the behavior of aliphatic hydroxyl groups under atmospheric-pressure ionization, in which protonation at the hydroxyl oxygen is followed by facile elimination of water and formation of a new carbon–carbon double bond. This loss is among the most abundant neutral losses associated with common functional groups and may already dominate the full-scan spectrum, causing the protonated molecule to be weak or absent (Holčapek *et al*., 2010; Levsen *et al*., 2007). The UV spectrum exhibited an absorption maximum at λmax = 205 nm, indicating the presence of a weakly conjugated olefinic system.

The IR spectrum displayed characteristic absorption bands at 3284.77, 3211.48, and 3105.39 cm^{-1}, corresponding to hydroxyl groups. Absorptions at 2985.81, 2949.16, 2922.16, 1469.76, 1444.32, and 1427.68 cm^{-1} were attributed to aliphatic C–H stretching and bending vibrations.

The ^1H and ^{13}C NMR spectra (Table 1) revealed three methyl groups, six methylene groups, five methine groups, two sp^3 quaternary carbons (C-5 and C-8), and four olefinic carbons, together with one oxygenated methylene (δC = 64.65) and two oxygenated methines (δC = 73.45 and 80.46). Signals at δC = 153.98 and 105.90 indicated an exomethylene group, whereas resonances at δC = 131.96 and 135.27 corresponded to a trisubstituted double bond. Because two of the five degrees of unsaturation are accounted for by these olefinic carbons, compound 1 was determined to possess a tricyclic skeleton.

The ^1H–^1H COSY spectrum showed couplings between the hydroxyl protons at δH = 6.06 (d, *J* = 3.2 Hz), 5.36 (d, *J* = 2.2 Hz), and 4.76 (t, *J* = 5.75 Hz) and the oxygenated protons at δH = 4.33 (H-9), 3.91 (H-7), and 3.75/3.78 (H-20), respectively, establishing the presence of two secondary hydroxyl groups and one primary hydroxyl group. Additional COSY correlations from H-10 (δH = 5.17) to H-12 and from H-7 to H_2-6 defined the connectivity around the seven-membered ring. In the HMBC spectrum, the vinylic methyl protons at δH = 1.69 (H-17) correlated with C-10 (δC = 131.96) and C-11 (δC = 135.27), locating the trisubstituted double bond, whereas the exomethylene protons at δH = 4.95 and 4.86 (H-19) correlated with C-18 (δC = 153.98). The strongly shielded methyl protons at δH = 0.78 (δC = 7.19) correlated with C-5, C-6, and C-7, placing this methyl group on a quaternary carbon adjacent to the

hydroxylated carbons. Such an unusually upfield methyl resonance has been attributed to the intramolecular shielding effect of two adjacent hydroxyl groups and is diagnostic of onychiol B (Xu *et al*., 1999). Key ^{1}H–^{1}H COSY and ^{1}H–^{13}C HMBC correlations of compound 1 are shown in Figure 1.

The ^{1}H and ^{13}C NMR data for compound 1 were in good agreement with those previously reported for onychiol B in pyridine-d_5. The small, uniformly upfield differences ($\Delta\delta \approx 1.0$ ppm) were consistent with the change in solvent to DMSO-d_6 (Xu *et al*., 1999). The IR absorptions at 3284.77, 3211.48, and 3105.39 cm^{-1} also agreed closely with the reported hydroxyl bands at 3280, 3220, and 3100 cm^{-1}. Thus, compound 1 was identified as onychiol B, a cyathane-type diterpenoid previously reported from *Onychium japonicum* (Hseu *et al*., 1980) and *O. lucidum* (Xu *et al*., 1999), and is reported here from the genus *Selliguea* for the first time.

Table 1. ^{1}H and ^{13}C (500 and 125 MHz) NMR data of compound 1 in DMSO-d_6

	Compound 1	
	δ_H (ppm), multiplicity, J [Hz]	δ_C (ppm) , type
1	1.52, m	50.45, CH
2	2.52, m	39.35, CH
3	2.08, m; 1.47, m	30.04, CH_2
4	1.53, m; 1.20, m	41.12, CH_2
5		44.37, C
6	1.60, m; 1.26, m	44.88, CH_2
7	3.91, m	73.45, CH
8		40.71, C
9	4.33, br s	80.46, CH
10	5.17, d, 2.2	131.96, CH
11		135.27, C
12	1.78, m; 1.52, m	33.67, CH_2
13	1.58, m; 1.13, m	23.40, CH_2
14	1.79, m	43.26, CH
15	1.02, s	21.99, CH_3
16	0.78, s	7.19, CH_3
17	1.69, s	25.37, CH_3
18		153.98, C
19	4.95, br s; 4.86, br s	105.90, CH_2
20	3.78, m; 3.75, m	64.65, CH_2
7-OH	5.36, d, 2.2	–
9-OH	6.06, d, 3.2	–
20-OH	4.76, t, 5.75	–

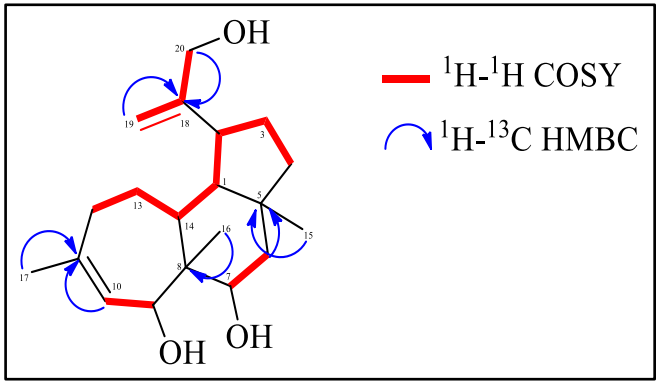


Figure 1. ^{1}H–^{1}H COSY and ^{1}H–^{13}C HMBC key correlations of compound 1

Compound 2 was obtained as yellow needles (m.p. 180–185 °C). Its negative-ion LC–MS spectrum showed a deprotonated molecule at *m/z* 431.15 $[M - H]^{-}$, consistent with the molecular formula $C_{21}H_{20}O_{10}$. The UV spectrum exhibited maxima at λmax = 204 nm (log ε = 4.582), 266 nm (log ε = 4.386), and 367 nm (log ε = 4.479). The position of band I at 367 nm is characteristic of a flavonol bearing a free 3-hydroxyl group. This assignment was supported by the ^{13}C resonances of C-2 (δC = 148.8) and C-3 (δC = 137.73), which are characteristic of an unsubstituted 3-OH group because 3-*O*-glycosylation shifts C-2 downfield to δC = 158–160 (Table 2). In the HMBC spectrum, the anomeric proton at δH = 5.55 (H-1″, d, *J* = 1.55 Hz) correlated with C-7 (δC = 163.45), establishing the position of the sugar, whereas no correlation was observed between an anomeric proton and C-3. The small anomeric coupling constant, together with the methyl doublet at δH = 1.26 (H-6″, *J* = 6.15 Hz, δC = 18.26), supported assignment of the sugar as an α-L-rhamnopyranosyl unit. Based on these data and comparison with published values, compound 2 was identified as kaempferol-7-*O*-α-L-rhamnoside (Aderogba *et al*., 2008).

Compound 3 was obtained as yellow needles (m.p. 202–203 °C). Its negative-ion LC–MS spectrum showed a deprotonated molecule at *m/z* 577.20 $[M - H]^{-}$, corresponding to the molecular formula $C_{27}H_{30}O_{14}$. The UV maxima at λmax = 205 nm (log ε = 4.549), 265 nm (log ε = 4.398), and 344 nm (log ε = 4.256) showed a hypsochromic shift of band I of approximately 23 nm relative to compound 2, indicating substitution at C-3. This interpretation was supported by the downfield shift of C-2 to δC = 159.9. Two anomeric protons were observed at δH = 5.39 (H-1″, d, *J* = 1.49 Hz, δC = 103.67) and 5.55 (H-1‴, d, *J* = 1.85 Hz, δC = 99.99), both with small coupling constants characteristic of α-L-rhamnopyranosyl units. Each was accompanied by a

methyl doublet at H-6″, with signals at δH = 0.90 (δC = 17.82) and 1.26 (δC = 18.22). The strongly shielded methyl signal at δH = 0.90 is characteristic of a rhamnosyl unit attached at C-3, where it lies above the B-ring, whereas the anomeric carbon at δC = 99.99 corresponds to the second rhamnosyl unit at C-7 and matches the value observed for compound 2. Thus, compound 3 was identified as kaempferol-3,7-*O*-α-L-dirhamnoside (Takaya *et al*., 2003).

Compound 4 was obtained as a yellow amorphous solid (m.p. 238–240 °C). Its negative-ion LC–MS spectrum showed a deprotonated molecule at *m/z* 593.15 $[M - H]^-$, consistent with the molecular formula $C_{27}H_{30}O_{15}$. The UV maxima at λmax = 205 nm (log ε = 4.459), 266 nm (log ε = 4.267), and 351 nm (log ε = 4.201) showed a hypsochromic shift of band I of approximately 16 nm relative to compound 2, consistent with substitution at C-3. This assignment was supported by the chemical shift of C-2 at δC = 158.0. Two anomeric protons were observed at δH = 5.63 (d, *J* = 1.45 Hz, δC = 99.62) and 5.53 (d, *J* = 7.3 Hz, δC = 101.98). The small coupling constant of the former, together with the methyl doublet at δH = 1.21 (*J* = 6.45 Hz, δC = 19.21), identified an α-L-rhamnopyranosyl unit, whereas the larger coupling constant of the latter, together with the oxygenated methylene signals at δH = 3.65 and 3.43 (δC = 62.31), indicated a β-D-glucopyranosyl unit. The anomeric carbon of the rhamnosyl unit (δC = 99.62) matched the value observed for the C-7 rhamnosides of compounds 2 and 3, placing this sugar at C-7 and, consequently, the glucosyl unit at C-3. All spectroscopic data were measured in the present study. The NMR data for compound 4 were recorded in DMSO-d_6, whereas those for compounds 2 and 3 were recorded in CD_3OD. The data agreed with those previously reported for this compound isolated from the rhizome of the same species (Baek *et al*., 1994). Thus, compound 4 was identified as kaempferol-3-*O*-β-D-glucoside-7-*O*-α-L-rhamnoside. Complete ^1H–^1H COSY, HSQC, and HMBC correlations for compounds 2–4 are provided in the supplementary material. The structures of compounds 2–4 are shown in Figure 2.

Table 2. ^1H and ^{13}C (500 and 125 MHz) NMR data of compound 2 and 3 in CD_3OD, and of compound 4 in DMSO-d_6

	Compound 2		Compound 3		Compound 4	
	δ_H, multiplicity, *J* [Hz]	δ_C, type	δ_H, multiplicity, *J* [Hz]	δ_C, type	δ_H, multiplicity, *J* [Hz]	δ_C, type
2		148.8, C		159.9, C		158.0, C
3		137.73, C		136.61, C		134.7, C

4		177.68, C		179.92, C		178.9, C
5		162.47, C		163.17, C		162.1, C
6	6.4, d, 2.1	100.09, CH	6.45, d, 2.3	100.67, CH	6.53, d, 2.0	100.6, CH
7		163.45, C		163.69, C		162.8, C
8	6.70, d, 2.1	95.45, CH	6.71, d, 2.3	95.75, CH	6.89, d, 2.0	95.7, CH
9		157.89, C		158.24, C		157.2, C
10		106.35, C		107.71, C		106.9, C
1'		123.69, C		122.55, C		122.0, C
2',6'	8.11, m	130.98, CH	7.79, m	132.18, CH	8.16, d, 8.85	132.2, CH
3',5'	6.91, m	116.51, CH	6.94, m	116.72, CH	6.98, d, 8.85	116.4, CH
4'		160.9, C		161.93, C		161.3, C
	7-O-α-L-Rhamnopyranosyl		3-O-α-L-Rhamnopyranosyl		7-O- α -L-Rhamnopyranosyl	
1"	5.55, d, 1.55	99.97, CH	5.39, d, 1.49	103.67, CH	5.63, d, 1.45	99.62, CH
2"	4.02, dd (1.5,3.5)	71.89, CH	4.22, dd, (1.7, 3.3)	72.05, CH	3.95, m	71.09, CH
3"	3.84, dd (3.5,9,4)	72.23, CH	3.72, dd, (3.35, 8.95)	72.24, CH	3.74, m	71.50, CH
4"	3.49, t 9.4	73.7, CH	3.35, m	73.30, CH	3.40, m	72.84, CH
5"	3.63, m	71.39, CH	3.35, m	71.00, CH	3.54, m	71.35, CH
6"	1.26, d, 6.15	18.26, CH3	0.9, d, 5.9	17.82, CH3	1.22, d, 6.45	19.21, CH_3
			7-O-α-L-Rhamnopyranosyl		3-O-β-D-Glucopyranosyl	
1'''			5.55, d, 1.85	99.99, CH	5.53, d, 7.3	101.98, CH
2'''			4.02, dd, (1.85, 3.45)	71.85, CH	3.30, m	75.47, CH
3'''			3.84, dd, (3.4, 9.4)	72.19, CH	3.32, m	77.68, CH
4'''			3.49, t, 9.4	73.72, CH	3.19, m	71.18, CH
5'''			3.62, m	71.43, CH	3.19, m	78.86, CH
6'''			1.26, d, 6.25	18.22, CH_3	3.65, m; 3.43, m	62.31, CH_2

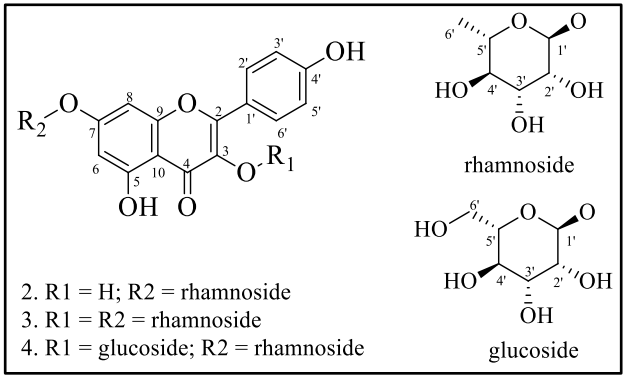


Figure 2. Structures of compounds 2 – 4

Three flavonol glycosides obtained in this study have previously been isolated from the unrelated plant *Bryophyllum pinnatum* (Crassulaceae) and evaluated against reference strains of *S. aureus* and *P. aeruginosa* using the broth microdilution method. In that study, α-rhamnoisorobin (kaempferol-7-*O*-α-L-rhamnoside, corresponding to compound 2) was the most active, with MIC values of 2 and 1 µg/mL, respectively, followed by kaempferol-3-*O*-glucopyranoside-7-*O*-α-L-rhamnopyranoside (4; 4 and 4 µg/mL) and kaempferitrin (3; 32 and 32 µg/mL) (Tatsimo *et al*., 2012). In the present evaluation against clinically relevant multidrug-resistant strains, onychiol B (1), kaempferol-3,7-*O*-α-L-dirhamnoside (3), and kaempferol-3-*O*-β-D-glucoside-7-*O*-α-L-rhamnoside (4) were inactive at 60 µg/disc. In contrast, compound 2 (kaempferol-7-*O*-α-L-rhamnoside) produced an inhibition zone of 12.17 ± 0.88 mm against MRSA and 6.92 ± 0.14 mm against MDRPA (Table 3). Because the reported zones include the 6 mm disc diameter, the inhibition halo against MDRPA extended only approximately 0.9 mm beyond the disc edge; thus, the effect against this organism was considered negligible. No qualitative potency categories were assigned because the assay was performed at a single concentration and no classification criterion was applied. The activity of compound 2 was considerably weaker than that of the positive control, chloramphenicol. No inferential statistical analysis was performed, and the values are presented descriptively.

The contrasting activities of the flavonol derivatives may point to a structure activity relationship (SAR) related to the glycosylation pattern, although the present data comprise only three flavonol glycosides tested at a single concentration. Compound 2, which carries a single rhamnosyl unit at C-7 and

a free 3-hydroxyl group, was the only active compound, whereas compounds 3 and 4, in which C-3 is also glycosylated, were inactive. No mechanistic experiments were carried out in this work, and the present data therefore do not allow the basis of this difference to be determined; the observation is reported here only as an association between the substitution pattern and the measured inhibition zones. A comparable association has been noted for kaempferol glycosides from other plant sources (Tatsimo *et al*., 2012). Flavonoids have also been reported to affect biofilm formation in *S. aureus* strains overexpressing efflux protein genes (Lopes *et al*., 2017), but no measurements of membrane permeability, target binding, or efflux activity were made in the present study. Establishing whether the glycosylation pattern is causally related to the activity would require quantitative assays across a larger set of analogues together with dedicated mechanistic studies.

Collectively, these findings identify compound 2 as the most active of the isolated compounds and therefore as the priority candidate for follow-up work. Before any structural modification is contemplated, the activity of compound 2 should first be quantified by determining its minimum inhibitory and minimum bactericidal concentrations against a panel of MRSA and MDRPA isolates, and its cytotoxicity against mammalian cells should be assessed in order to establish a selectivity index. Should these data confirm a useful level of activity, subsequent studies could address the mechanism of action and explore structural analogues.

This study provides new chemical and biological information on *S. feei* and further supports its potential as a source of bioactive secondary metabolites. Continued investigation of its phytochemical diversity and biological activity may identify additional compounds of interest for antimicrobial drug development.

4. Conclusions and Recommendations

Phytochemical investigation of the fronds of *S. feei* Bory (Polypodiaceae) yielded one diterpenoid, onychiol B (1), and three flavonol glycosides, kaempferol-7-*O*-α-L-rhamnoside (2), kaempferol-3,7-*O*-α-L-dirhamnoside (3), and kaempferol-3-*O*-β-D-glucoside-7-*O*-α-L-rhamnoside (4). None of the four compounds is structurally new; however, compounds 1–3 are reported for the first time from the genus *Selliguea*, extending the known chemical diversity of Polypodiaceae ferns to their aerial organs. Antibacterial

evaluation against clinically relevant multidrug-resistant strains demonstrated that compound 2 produced inhibition zones of 12.17 ± 0.88 mm against MRSA and 6.92 ± 0.14 mm against MDRPA at 60 µg/disc, whereas compounds 1, 3, and 4 were inactive at the same concentration. Among the flavonol glycosides examined, activity was observed only for the compound carrying a single rhamnosyl unit at C-7 without additional substitution at C-3; whether this substitution pattern is causally related to the activity was not established in this study. These findings establish the fronds of *S. feei* as a chemically productive plant organ warranting further investigation and identify compound 2 as the priority candidate for follow-up work, beginning with the determination of its minimum inhibitory and minimum bactericidal concentrateeons and its cytotoxicity.

5. Acknowledgement

The authors gratefully acknowledge the Competency Grant 2015-217 and 2018 DP2M-DIKTI- The ministry of Research, Technology and Higher Education of the Republic of Indonesia to DA. We thank M. Djamil Hospital, Padang; Cipto Mangunkusumo Hospital, Jakarta; and Microbiology Laboratory Fac. of Medicine – Andalas University for providing the testing microbes; to Dr. Nurainas from Andalas University Herbarium (ANDA) for identification of the herbarium specimen and to Prof. Dr. Matthias Hamburger and Dr. Ombeline Danton from Pharmaceutical Biology, the University of Basel for NMR and MS measurements.

6. References

Aderogba, M. A., McGaw, L. J., Ogundaini, A. O., & Eloff, J. N. (2008). Cytotoxicity Study of Antioxidant Flavonoids from *Bauhinia tomentosa* leaf extract. *Nigerian Journal of Natural Products and Medicine, 12*, 50–54. https://doi.org/10.4314/njnpm.v12i1.45670

Anggia, V., Bakhtiar, A., & Arbain, D. (2015). Chemical constituents and antibacterial activities of leaves of Sumatran King Fern (*Angiopteris evecta* G. Forst HOFFM.). *Jurnal Farmasi Indonesia, 7*(4), 195–202. https://doi.org/10.35617/jfi.v7i4.193

Baek, N.-I., Chung, M.-S., Shamon, L., Kardono, L. B. S., Tsauri, S., Padmawinata, K., Pezzuto, J. M., Soejarto, D. D., & Kinghorn, A. D. (1993). *Selligueain A*, a Novel

Highly Sweet Proanthocyanidin from the Rhizomes of *Selliguea feei*. *Journal of Natural Products, 56*(9), 1532–1538. https://doi.org/10.1021/np50099a011

Baek, N.-I., Kennelly, E. J., Kardono, L. B. S., Tsauri, S., Padmawinata, K., Soejarto, D. D., & Kinghorn, A. D. (1994). Flavonoids and a proanthocyanidin from rhizomes of *Selliguea feei*. *Phytochemistry, 36*(2), 513–518. https://doi.org/10.1016/S0031-9422(00)97105-X

Handayani, D., Aminah, I., Putra, P., Putra, A. E., Arbain, D., Satriawan, H., Efdi, M., Celik, I., & Tallei, T. E. (2023). The depsidones from marine sponge-derived fungus Aspergillus unguis IB151 as an anti-MRSA agent: Molecular docking, pharmacokinetics analysis, and molecular dynamic simulation studies. *Saudi Pharmaceutical Journal*, *31*, 1–9. https://doi.org/10.1016/j.jsps.2023.101744

Holčapek, M., Jirásko, R., & Lísa, M. (2010). Basic rules for the interpretation of atmospheric pressure ionization mass spectra of small molecules. *Journal of Chromatography A, 1217*(25), 3908–3921. https://doi.org/10.1016/J.CHROMA.2010.02.049

Hseu, T. H., Wang, J. L., & Tang, C. P. (1980). The structure of onychiol B, [1aS,3aS-(1β,1aα,3aβ,5α,5aα,6α,10aβ)]-1-[1-(hydroxymethyl)vinyl]-3a,5a,8-trimethyl-2,3,3a,4,5,5a,9,10,10a,10b-decahydro-1H,6H-cyclohept[e]indene-5,6-diol: a diterpene alcohol from *Onychium japonicum* (Thunb.) Kunze. Acta Crystallographica Section B, 36(11), 2802–2804. https://doi.org/10.1107/S0567740880010096

Levsen, K., Schiebel, H.-M., Terlouw, J. K., Jobst, K. J., Elend, M., Preiß, A., Thiele, H., & Ingendoh, A. (2007). Even-electron ions: a systematic study of the neutral species lost in the dissociation of quasi-molecular ions. *Journal of Mass Spectrometry*, *42*(8), 1024–1044. https://doi.org/https://doi.org/10.1002/jms.1234

Liao, G., Mo, L., Teng, M., Xiong, X., Xu, X., Liu, J., & Lu, R. (2023). Japonins A–D, cyathane diterpenoids with neurite outgrowth-promoting activity isolated from Onychium japonicum using NMR and MS/MS-based molecular networking. *Fitoterapia*, *170*, 105632. https://doi.org/10.1016/J.FITOTE.2023.105632

Lopes, L. A. A., dos Santos Rodrigues, J. B., Magnani, M., de Souza, E. L., & de Siqueira-Júnior, J. P. (2017). Inhibitory effects of flavonoids on biofilm formation by *Staphylococcus aureus* that overexpresses efflux protein genes. *Microbial Pathogenesis*, *107*, 193–197. https://doi.org/10.1016/j.micpath.2017.03.033

Nofrizal, Putra, D. P., & Arbain, D. (2017). Antioxidant and Antibacterial Constituents from Two Sumatran Ferns, *Trichomanes javanicum* and *Oleandra pistillaris*. *Natural Product Communications*, *12*(8), 1263–1264. https://doi.org/10.1177/1934578x1701200829

Subarnas, A., & Wagner, H. (2000). Analgesic and anti-inflammatory activity of the *proanthocyanidin selligueain* A from *Polypodium feei* METT. *Phytomedicine : International Journal of Phytotherapy and Phytopharmacology, 7*(5), 401–405. https://doi.org/10.1016/S0944-7113(00)80061-6

Syafni, N., Putra, D. P., & Arbain, D. (2012). 3,4-dihydroxybenzoic acid and 3,4-dihydroxybenzaldehyde from the fern *Trichomanes chinense* L.; isolation, antimicrobial and antioxidant properties. *Indonesian Journal of Chemistry, 12*(3), 273–278. https://doi.org/10.22146/ijc.21342

Takaya, Y., Kondo, Y., Furukawa, T., & Niwa, M. (2003). Antioxidant Constituents of Radish Sprout (Kaiware-daikon), *Raphanus sativus* L. Journal of Agricultural and Food Chemistry, 51(27), 8061–8066. https://doi.org/10.1021/jf0346206

Tatsimo, S. J. N., Tamokou, J. D. D., Havyarimana, L., Csupor, D., Forgo, P., Hohmann, J., Kuiate, J. R., & Tane, P. (2012). Antimicrobial and antioxidant activity of *kaempferol rhamnoside* derivatives from *Bryophyllum pinnatum*. *BMC Research Notes, 5*, 158. https://doi.org/10.1186/1756-0500-5-158

Valgas, C., de Souza, S. M., Smânia, E. F. A., & Smânia Jr., A. (2007). Screening methods to determine antibacterial activity of natural products. *Brazilian Journal of Microbiology, 38*, 369–380. https://doi.org/10.1590/S1517-83822007000200034

Xu, Y., Zheng, X. & He, Y.N. (1999). Flavonoids of *Onychium lucidum*. *Acta Botanica Yunnanica*, *21*(4), 497–504.